

Kinetics and Mechanism of the Dehydration Reaction of Sarcosine to a Bislactame through Diacylperoxide Intermediate in Strong Acidic Medium

HOMAYOON BAHRAMI,^{1,2} MEHDI D. DAVARI,¹ MARYAM KESHAVARI,¹ MANSOUR ZAHEDI,¹ AYOOB BAZGIR,¹ ALI A. MOOSAVI-MOVAHEDI²

¹Department of Chemistry, Faculty of Sciences, Shahid Beheshti University, Evin, P.O. Box 19395-4716, Tehran 19839-6313, Iran

²Institute of Biochemistry and Biophysics, University of Tehran, Tehran, Iran

Received 12 November 2008; accepted 23 May 2009

DOI 10.1002/kin.20441

Published online in Wiley InterScience (www.interscience.wiley.com).

ABSTRACT: The influence of substitution on the amine functional group of glycine in the permanganic oxidation of such an α -amino acid in moderately concentrated sulfuric acid medium has been investigated. Reaction products analysis has revealed that contrary to the usual α -amino acid oxidation product, which is an aldehyde species, a valuable compound, namely 1,4-dimethylpiperazine-2,5-dione, has been obtained as the main product via a cheap, simple, efficient, and novel method. Sarcosine has been chosen as a substituted derivative of glycine, and the kinetics and mechanism of its permanganic oxidation have been investigated using a spectrophotometric technique. Conclusive evidence has proven delayed autocatalytic activity for Mn(II) in this reaction, analogous to some α -amino acids. It has been revealed that such activity can show up when a certain concentration ratio of Mn(II) to sarcosine is built up in the medium, which we call the "critical ratio." The magnitude of the latter ratio depends on the sulfuric acid concentration. Considering the "delayed autocatalytic behavior" of Mn(II) ions, rate equations satisfying observations for both catalytic and noncatalytic routes have been presented. The reaction shows first-order dependence on permanganate ions and sarcosine concentrations in both catalytic and noncatalytic pathways, and apparent first-order dependence on Mn²⁺ ions in catalytic pathways. The correspondence of pseudo-order rate constants

Correspondence to: Mansour Zahedi; e-mail: m-zahedi@cc.sbu.ac.ir.

Contract grant sponsor: Research Council of Shahid Beheshti University.

© 2009 Wiley Periodicals, Inc.

of the catalytic and noncatalytic pathways to Arrhenius and Eyring laws has verified "critical ratio" as well as "delayed autocatalytic behavior" concepts. The activation parameters associated with both pathways have been computed and discussed. Mechanisms for both catalytic and noncatalytic routes involving radical intermediates as well as a product having a diketopiperazine skeleton have been reported for the first time. © 2009 Wiley Periodicals, Inc. *Int J Chem Kinet* 41: 689–703, 2009

INTRODUCTION

Monomeric sarcosine oxidase (MSOX) and *N*-methyltryptophan oxidase (MTOX) catalyze similar oxidative reactions with various secondary or tertiary amino acids. MSOX catalyzes oxidative demethylation of sarcosine (*N*-methylglycine) and other secondary amino acids such as L-proline, to yield glycine, formaldehyde, and hydrogen peroxide. Sarcosine is a common soil metabolite that can act as the sole source of carbon and energy for many microorganisms. Despite the sequence similarity with MSOX, sarcosine is a very poor substrate for *N*-methyltryptophan oxidase (MTOX), which exhibits a preference for aromatic or large aliphatic *N*-methylated amino acids [1–4].

A new survey shows that diketopiperazines (DKPs) are very important and attractive synthetic targets because of their wide range of interesting biological activity and their presence in a wide variety of natural products [5–7]. Synthetically, DKPs have been used as a starting material for the preparation of enantiomerically pure compounds, as chiral auxiliaries in asymmetric synthesis such as the asymmetric Diels–Alder reaction [8–10]. DKPs have also been shown to catalyze some additional organic reactions [11–14].

The synthesis of this class of compounds has already been reported. Several methods have been reported for the synthesis of DKPs. However, these methods suffer from several limitations. They require harsh conditions, volatile unfriendly organic solvents, long reaction times, and low yields [11–14]. Owing to the above reasons and as a part of our ongoing research program on oxidation of amino acids [15–17], we have developed a simple approach for producing this important class of diketopiperazine-2 (Scheme 1). A literature survey shows that the kinetics and mechanism of oxidation of amino acid in moderately concentrated acid medium have been extensively studied [15–31]. In most of these studies, the reaction has been considered as a process that follows a perfect second-order kinetics at constant $[H^+]$ without any autocatalytic effect. There are two reports of a "double stage" process in which every stage is shown to have kinetics identical to a pseudo-first-order reaction [27,31]. In our previous studies [15,16], we have reported the presence of the autocatalytic effect in which Mn^{2+} is the autocatalytic

agent, whereas in a recent work it is shown that such autocatalytic activity is accompanied by a delay and it shows up just after a critical ratio of Mn(II) to amino acid is built up, depending on the nature of the amino acid used [17].

As an attempt to investigate the effect of amine's substitution of an α -amino acid in permanganate oxidation, we have chosen sarcosine. Besides the importance of the kinetic and mechanism study of such a process, product analysis has revealed that permanganic oxidation of sarcosine can be regarded as a novel method for the synthesis of a valuable diketopiperazine skeleton. The advantages of such synthesis can be stated as having a smooth condition, water as solvent, high yield, and a single-step procedure.

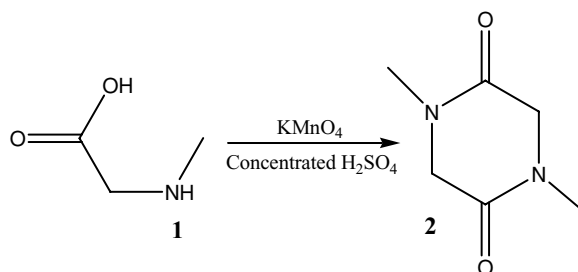
EXPERIMENTAL

Materials

All the reagents were from Merck or Fluka. All reagents were of analytical grade, and their solutions were prepared by dissolving the requisite amount of samples in tridistilled, deionized, and boiled water. All weighting was performed by a Shimadzu AW220 electronic balance (± 0.0001 g). The preparation and analysis of the stock solutions and process for kinetic runs were the same as described earlier [15–17]. The permanganate solutions were prepared and tested by the Vogel method [32].

Kinetic Measurements

The kinetic progress of reaction was followed by measuring the absorbance of the permanganate ions at 525 nm (maximum wavelength for permanganate ions in a strong acid solution) with a thermostated (Shimadzu TB-85, ± 0.1 K) Shimadzu (1605 model) UV–vis spectrophotometer within the temperature range of 25–65°C. It was verified that there is no interference from other reagents at this wavelength. The molar absorption coefficient for permanganate of $2.26 \times 10^3 \text{ dm}^3 \text{ mol}^{-1} \text{ cm}^{-1}$ was obtained and was used in all kinetic measurements presented in this work. Sarcosine was used in an excess amount relative to



Scheme 1

permanganate. To follow up the reaction, TLC was carried out on precoated plates, and spots were detected by UV light. The melting point was taken on an electrothermal 9200 point apparatus and left uncorrected. The IR spectra were obtained in potassium bromide pellets with a Shimadzu IR-470 spectrometer. The ^1H NMR and ^{13}C NMR spectra were taken by a Bruker Avance DPX300 spectrometer in CDCl_3 , and chemical shifts are in ppm relative to CDCl_3 . A Shimadzu QP-1100EX mass spectrometer with electron impact ionization mode was used to measure the MS data.

Products Analysis

To analyze and identify the reaction products, oxidation of sarcosine was performed at constant temperature in acidic medium. In the course of reaction, the solution's color changed from violet to colorless, indicating Mn^{2+} ion generation as the major manganese moiety. Oxygen gas was generated during the reaction, and a conclusive flame test confirmed O_2 generation. After completion of the reaction, the products were isolated and identified using IR, ^1H NMR, ^{13}C NMR, and MS spectra as well as melting points. The main product (1,4-dimethylpiperazine-2,5-dione) that was isolated is a dimer of two sarcosine molecules having a diketopiperazine skeleton, which is reported for the first time. It is noteworthy that, as expected, no CO_2 gas was detected as a product of the reaction, due to the presence of two carbonyl groups in the major product. Despite the usual synthetic routes for producing this important class of 2,5-diketopiperazines [11–14], a simple single step oxidation process in aqueous medium, high yield, mild conditions has afforded the mentioned product. Thus, a significant result of this paper is to replace environmentally unfriendly organic solvents with environmentally friendly H_2O , to omit organic solvents, and to increase reaction rates and product yields. This cyclization process is presented in Scheme 1.

Procedure for Direct Synthesis of Product

A solution of sarcosine (0.222 g, 2.5 mmol), KMnO_4 (0.078 g, 0.5 mmol), concentrated H_2SO_4 (98%) (3.16 mol dm^{-3}), was stirred for 8 h until the solution of KMnO_4 became colorless. At the end of the reaction, the solution was neutralized with barium hydroxide. The neutralization process must be done slowly for 2 h, so that the heat of the neutralization reaction does not affect the product. The organic phase is subsequently distilled under vacuum condition. The sole organic product was approved by a single spot on TLC. The residual was extracted with chloroform and was crystallized with chloroform and *n*-hexane. The yield calculated amounts to 80%. An analysis of the product gave the following results:

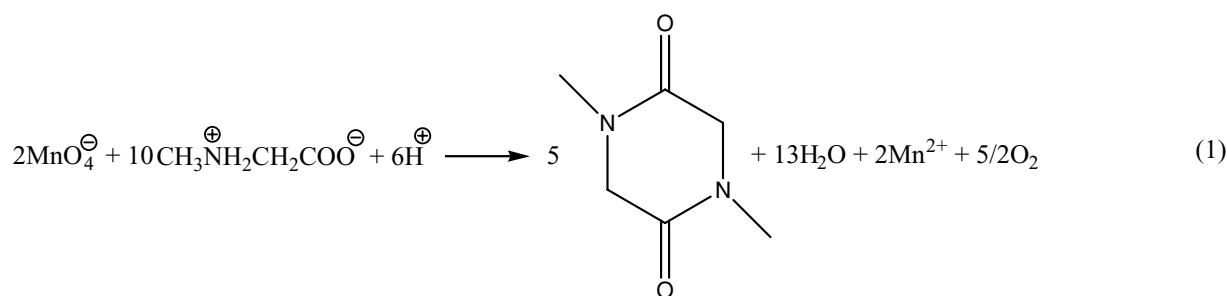
1,4-Dimethylpiperazine-2,5-dione: White crystals; mp 143–145°C; IR (KBr) 2961 (C–H, aliphatic), 1657 (C=O), 1334 (CO–N), 1015 (C–N) cm^{-1} ; ^1H NMR (300 MHz, CDCl_3) δ : 2.98 (6H, s, 2 CH_3), 3.48 (4H, s, 2 CH_2), ^{13}C NMR (75 MHz, CDCl_3) δ : 33.27 (CH_3), 51.63 (CH_2), 163.08 (CON); MS (m/z): 143 (M + H, 85), 142 (M, 75), 113 (M-24, 46), 85, 57 (100).

^1H NMR is ordered as follow: proton numbers, multiplicity (s, singlet; d, doublet; t, triplet; q, quartet; m, multiplet), and group.

The study reveals that the ^{13}C NMR spectrum has three types of carbons, whereas the MS spectrum verifies that the compound mass is equal to the proposed product. As an assurance, it was observed that when an oxidizing agent, namely permanganate, was removed from the medium, no cyclization could occur, meaning that sulfuric acid alone cannot lead to the product and permanganate presence is obligatory. As another test of confidence, the reaction was performed with Mn(II) when KMnO_4 was absent, and as a result no observable product was detected.

Reaction Stoichiometry

Reaction mixtures containing various ratios of sarcosine to MnO_4^- were mixed in the presence of 3.16 mol dm^{-3} H_2SO_4 and then equilibrated for 24 h at room temperature. Estimation of the unreacted MnO_4^- showed that 1 mol of MnO_4^- consumed 5 mol of amino acid to produce 2.5 mol of 1,4-dimethylpiperazine-2,5-dione as the major product [29]. In view of these results and taking into account that the final product of permanganate reduction in an acid medium and in a large excess of reducing species is the Mn^{+2} ion [18,20,28,33], the following equation was obtained:



Acrylonitrile Addition

The reaction mixture was mixed with acrylonitrile monomer and was kept for 2 h in an inert atmosphere. The presence of free radicals as intermediates was confirmed by polymerization, both in the presence and in the absence of manganese sulfate(II). The blank experiments of either MnO_4^- or sarcosine alone with acrylonitrile did not induce polymerization under the same conditions as those induced with reaction mixtures. Initially added acrylonitrile decreases the rate, indicating the free radical intervention, which is the case in earlier work [15–31].

RESULTS AND DISCUSSION

Rate Equation

Figure 1 illustrates the permanganate absorption vs. wavelength curves for sarcosine oxidation, obtained at 10 min intervals as the reaction proceeded. In the course of the permanganate oxidation process, it is ev-

ident that the Mn(VII) is reduced to various states in acidic, alkaline, and neutral media. Furthermore, the mechanism by which this multivalent oxidant oxidizes a substrate depends not only on the substrate but also on the medium [34] used for the study. In a strongly acidic medium, the stable reaction product is the Mn^{2+} ion. From previous studies [35–43], it is known that MnO_2 absorbs in the 400–650 nm region, so the absorption profiles suggest that MnO_2 is not a reaction product. Furthermore, since no rise and fall in absorption is observed at 418 nm, it is concluded that MnO_2 does not intervene as a possible oxidizing agent unless it is short lived. Furthermore, the maximum absorption wavelengths for Mn(IV) and Mn(III) ions lie in the 400–460 nm region. It has been reported that permanganate absorption at the maximum wavelength of the aforementioned species is about 0.458 and 0.108 of its absorption at 525 nm (permanganate λ_{max}) [44]. Thus, if Mn(IV) and Mn(III) species existed as stable moieties in the reaction medium, the absorption profile of permanganate with time must have changed from what was observed in Fig. 1 in order to contain the

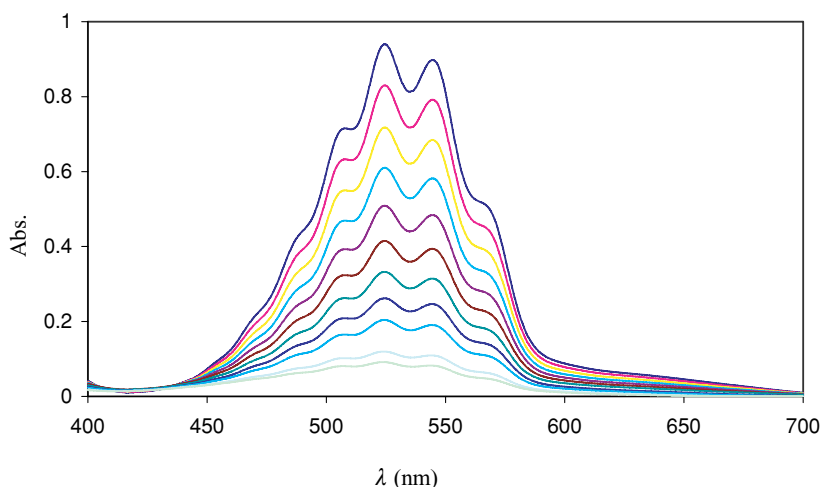


Figure 1 Spectral changes in the oxidation of sarcosine with permanganate ions. $[\text{KMnO}_4] = 4.0 \times 10^{-4} \text{ mol dm}^{-3}$, $[\text{Sar}] = 0.05 \text{ mol dm}^{-3}$, $[\text{H}_2\text{SO}_4] = 3.16 \text{ mol dm}^{-3}$, $T = 323 \text{ K}$, and scanning time intervals = 10 min. [Color figure can be viewed in the online issue, which is available at www.interscience.wiley.com.]

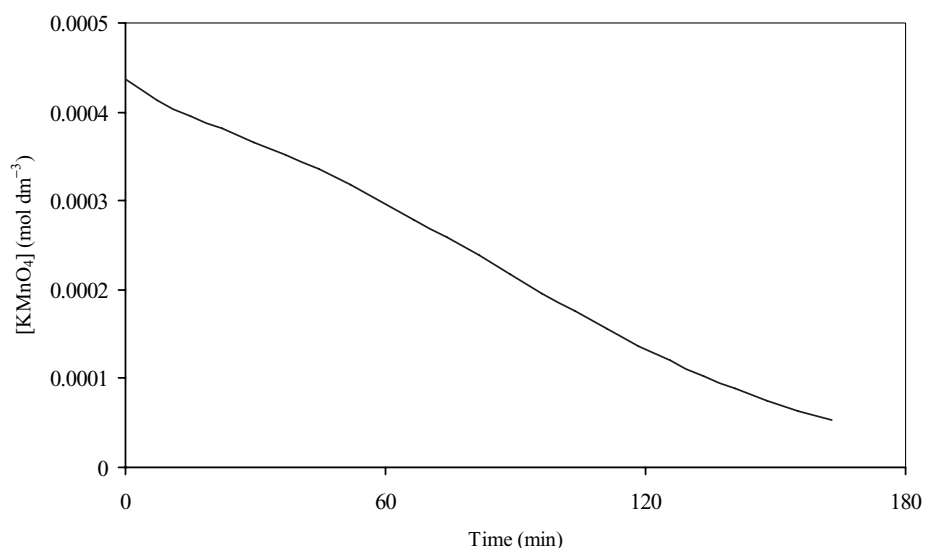


Figure 2 Concentration changes vs. time plot. $[\text{KMnO}_4] = 4.0 \times 10^{-4} \text{ mol dm}^{-3}$, $[\text{H}_2\text{SO}_4] = 3.16 \text{ mol dm}^{-3}$, $[\text{Sar}] = 0.05 \text{ mol dm}^{-3}$, $T = 318 \text{ K}$.

former ion absorption features. It is worth mentioning here that for Mn(III) to be generated as a product of the direct reaction between permanganate and Mn(II), an acidic medium with a pH of about 1–2 is required [45]. Also it has been reported that for Mn(III) to become stable in the latter medium, species such as $\text{C}_2\text{O}_4^{2-}$ [46] and $\text{P}_2\text{O}_7^{4-}$ [47] are necessary. Therefore, it is concluded that under our present conditions, Mn(IV) and Mn(III) ions can neither be yielded via the direct

permanganate-Mn(II) reaction, nor they are stable even if they are generated by the amino acid–permanganate reaction.

In Fig. 2, a typical permanganate concentration change vs. time plot has been shown. Since Fig. 2 does not appear to be a perfect sigmoidal profile, it might be judged that an autocatalysis reaction has not occurred, which may lead to erroneous results. However, taking a closer look at the rate–time plot of Fig. 3, a bell-shaped

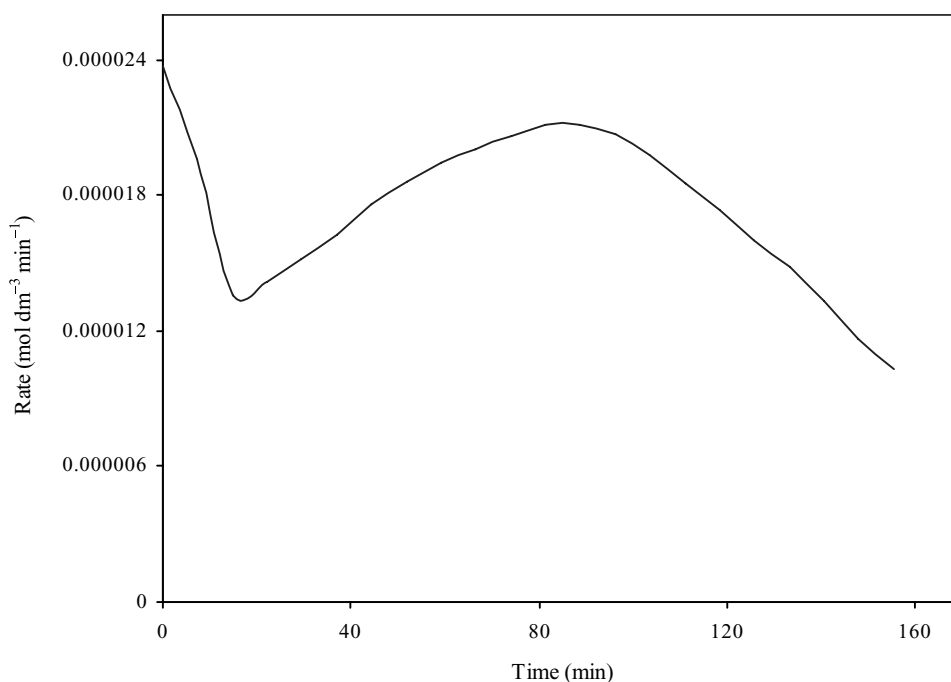


Figure 3 Reaction rate vs. time plot. $[\text{KMnO}_4] = 4.0 \times 10^{-4} \text{ mol dm}^{-3}$, $[\text{H}_2\text{SO}_4] = 3.16 \text{ mol dm}^{-3}$, $[\text{Sar}] = 0.05 \text{ mol dm}^{-3}$, $T = 318 \text{ K}$.

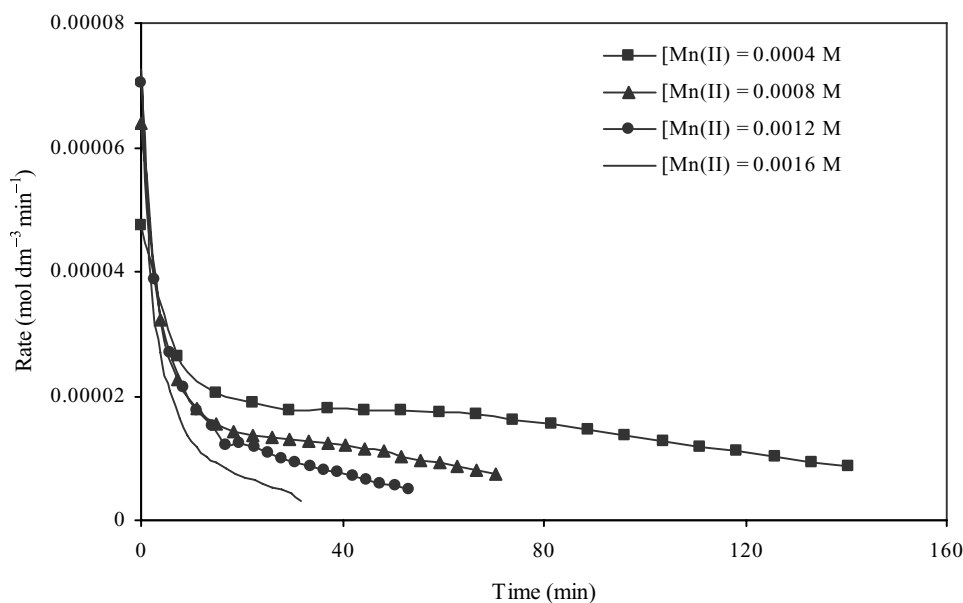


Figure 4 Effect of the added initial concentration of Mn^{2+} ions on the reaction rate–time plots. $[\text{Sar}] = 0.05 \text{ mol dm}^{-3}$, $[\text{KMnO}_4] = 4.0 \times 10^{-4} \text{ mol dm}^{-3}$, $[\text{H}_2\text{SO}_4] = 3.16 \text{ mol dm}^{-3}$, $T = 303 \text{ K}$.

curve can be seen after 35% of the reaction progression. Such an observation is clear evidence of a delayed autocatalytic behavior for this reaction as has been reported elsewhere [17].

Figure 4 illustrates the rate of permanganate concentration change vs. time curves in the order of increasing initial concentration of $\text{Mn}(\text{II})$. Considering Fig. 4, it is obvious that the reaction's half life has been decreased by adding increasing amounts of Mn^{2+} . In addition, the increasing rate portion (bell shaped) of these curves is gradually annihilated, while the Mn^{2+} concentration has been increased to 0.0016 M. Thus, from above observations it could be concluded that Mn^{2+} is the autocatalytic agent. As has been reported before [17] and is evidenced from Figs. 3 and 4, for Mn^{2+} to show such “delayed autocatalytic characteristic,” it should acquire a certain concentration, which we call “critical concentration.” It should be noted that some experiments were carried out with all reactants, namely KMnO_4 , $\text{Mn}(\text{II})$, and H_2SO_4 , while amino acid was absent. The result was that the permanganate rate of consumption was much slower than when sarcosine was present. This observation confirms that permanganate consumption can be due to the amino acid oxidation rather than direct permanganate reaction with $\text{Mn}(\text{II})$, which is known to be very slow. Thus regarding the product analysis section, generation of 1,4-dimethylpiperazine-2,5-dione can be understood only by a direct reaction between sarcosine and permanganate, which is catalyzed by $\text{Mn}(\text{II})$ ions as shown above.

According to the above discussion, the following rate equation is proposed for sarcosine oxidation until the autocatalytic behavior of Mn^{2+} emerges:

$$-\frac{d[\text{MnO}_4^-]}{dt} = k'_1[\text{MnO}_4^-] \quad (2)$$

As the reaction progresses, the following equation for sarcosine is yielded:

$$-\frac{d[\text{MnO}_4^-]}{dt} = k'_1[\text{MnO}_4^-] + k'_2[\text{MnO}_4^-][\text{Mn}^{2+}] \quad (3)$$

where k'_1 and k'_2 are pseudo-order rate constants for the noncatalytic and catalytic processes, respectively. The sarcosine concentration, which is always kept in large excess, and the constant sulfuric acid concentration in each experiment are included in these pseudo-order rate constants. The integrated form of the equations gives

$$\ln \frac{a}{(a-x)} = k'_1 t \quad (4)$$

$$\ln \frac{k'_1/k'_2 + x}{a-x} = (k'_1 + k'_2 a)t - \ln \frac{k'_2 a}{k'_1} \quad (5)$$

where a represents the initial concentration of permanganate and x is the amount of permanganate ion consumed in time t .

Initial anticipation of k'_1 for sarcosine has been made by fitting the early portion of the rate data to a first-order rate equation. This is because there is no

Table I Rate Constants for the Catalyzed and Uncatalyzed Processes at Different Temperatures

| T (K) | $k'_1 \times 10^5$ (s^{-1}) | $k'_2 \times 100$ ($dm^3 mol^{-1} s^{-1}$) |
|---------|---------------------------------|--|
| 298 | 1.52 | 6.75 |
| 303 | 2.07 | 14.42 |
| 308 | 3.28 | 27.69 |
| 313 | 4.5 | 43.98 |
| 318 | 6.11 | 71.33 |
| 323 | 9.01 | 106.68 |
| 328 | 13.49 | 155.66 |
| 333 | 21.85 | 241.07 |
| 338 | 33.54 | 403.99 |

$[KMnO_4] = 4.0 \times 10^{-4} mol dm^{-3}$, $[H_2SO_4] = 3.16 mol dm^{-3}$, $[Sar] = 0.05 mol dm^{-3}$. Estimated errors on each of k'_1 are 1%–2% and k'_2 are 0.5%–1%.

catalytic effect in the early stages of the reaction. Having anticipated preliminary values of k'_1 and k'_2 , Eq. (5) has been used for the simultaneous determination of the kinetic data of the reaction rate increase region, by taking advantage of iterative methods [15–17,35–43,48–53], and such data are summarized in Table I. Figure 5 demonstrates the typical results of the fitting process of the rate data for sarcosine at various temperatures and under the same conditions. Almost perfect fits to the data in Fig. 5 (R^2 values of 0.9991–0.9993) not only corroborate the validity of the applied kinetics method but also confirm the autocatalytic effect of the Mn^{2+} species and point to such delayed activity at

Table II Rate Constants for the Catalyzed and Uncatalyzed Processes Accompanied by Thresholds (%) for the Appearance of the Autocatalysis Behavior at Different Concentrations of Sarcosine

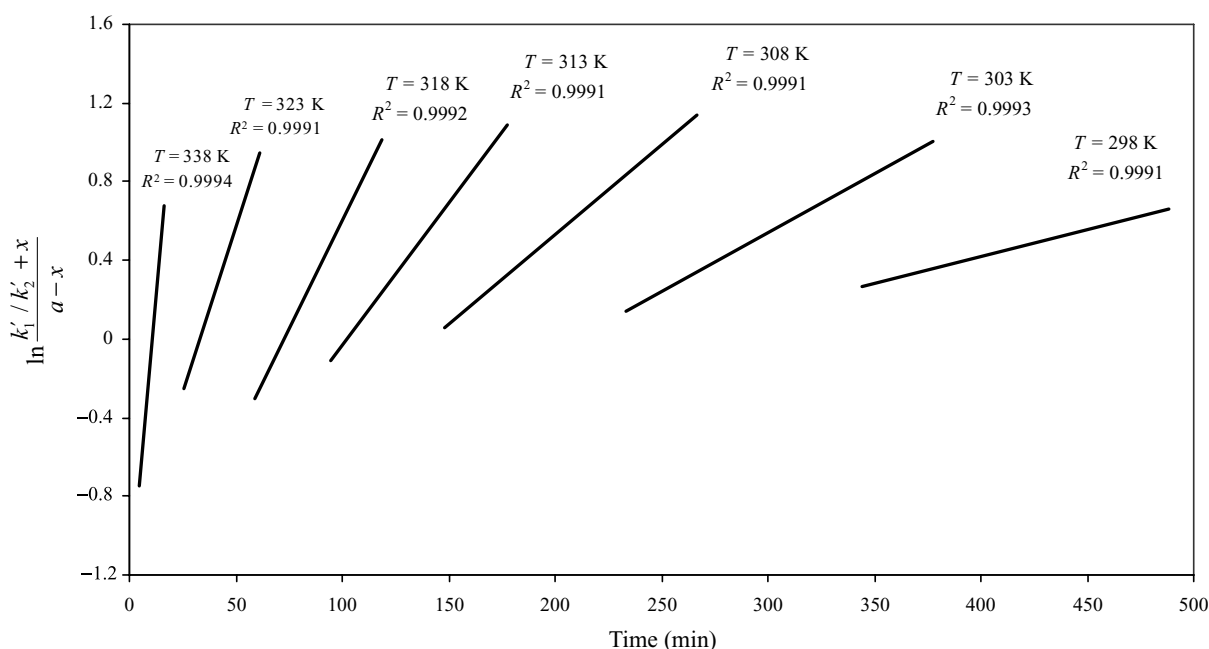
| [Sar] ($mol dm^{-3}$) | $k'_1 \times 10^5$ (s^{-1}) | $k'_2 \times 100$ ($dm^3 mol^{-1} s^{-1}$) | Reaction Progress (%) |
|-------------------------|---------------------------------|--|-----------------------|
| 0.03 | 4.29 | 40.56 | 17 |
| 0.04 | 5.88 | 53.25 | 23 |
| 0.05 | 7.33 | 71.33 | 32 |
| 0.06 | 10.11 | 89.98 | 34 |
| 0.07 | 11.53 | 102.56 | 37 |
| 0.09 | 15.49 | 132.57 | 38 |

$[KMnO_4] = 4.0 \times 10^{-4} mol dm^{-3}$, $[H_2SO_4] = 3.16 mol dm^{-3}$, $T = 318 K$.

certain critical concentrations of Mn^{2+} . Note that estimated errors on k'_1 and k'_2 are 1%–2% and 0.5%–1% throughout all experiments, respectively.

Dependence of Reaction Rate on [Sar]

Figure 6a illustrates rate–time curves of the reaction in different concentrations of sarcosine. Considering Fig. 6, it is clear that onset of the autocatalytic activity is further delayed if sarcosine concentration is increased. Such a fact can be justified by referring to the data of Table II. It can, therefore, be concluded that the initiation of autocatalytic activity depends not only on

**Figure 5** Integrated rate-law plots for the oxidation of sarcosine by potassium permanganate at various temperatures. $[Sar] = 0.05 mol dm^{-3}$, $[KMnO_4] = 4.0 \times 10^{-4} mol dm^{-3}$, $[H_2SO_4] = 3.16 mol dm^{-3}$.

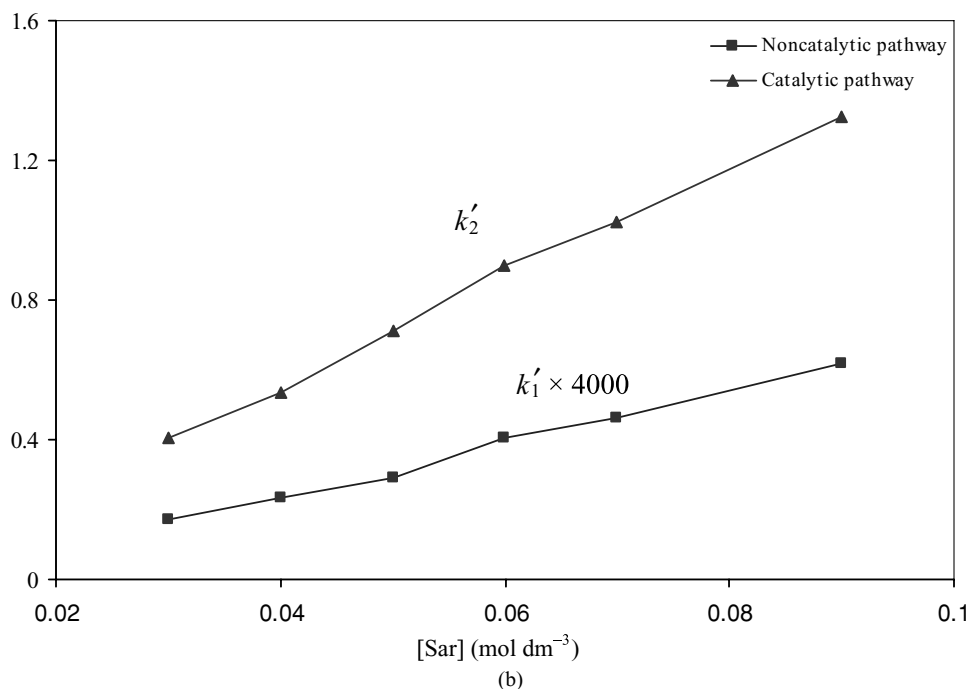
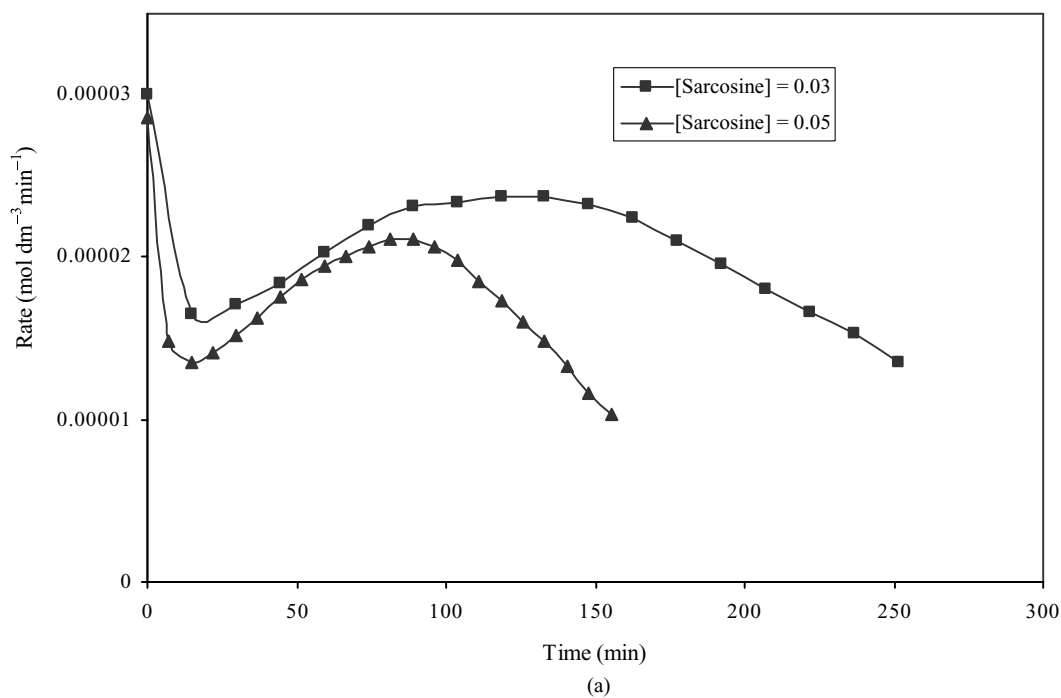


Figure 6 Effect of sarcosine concentration on (a) the reaction rate–time plots and (b) the catalyzed and uncatalyzed pseudo-order rate constants. $[\text{KMnO}_4] = 4.0 \times 10^{-4} \text{ mol dm}^{-3}$, $[\text{H}_2\text{SO}_4] = 3.16 \text{ mol dm}^{-3}$, $T = 318 \text{ K}$; $k'_1 \text{ (s}^{-1}\text{)}$, $k'_2 \text{ (dm}^3 \text{ mol}^{-1} \text{ s}^{-1}\text{)}$.

the Mn^{2+} concentration but also on that of sarcosine. Thus, the delayed autocatalytic effect can occur only at certain concentrations of Mn^{2+} to sarcosine, namely the “critical ratio.”

The pseudo-order rate constants obtained at various sarcosine concentrations are shown in Fig. 6b. Plots of $\ln(k'_1)$ and $\ln(k'_2)$ against $\ln[\text{Sar}]$ (not shown) confirm that the reaction order can be considered to be equal

Table III Rate Constants for the Catalyzed and Uncatalyzed Processes Accompanied by Thresholds (%) for Appearance of Autocatalysis Behavior at Different Concentrations of Sulfuric Acid

| [H ₂ SO ₄] (mol dm ⁻³) | $k'_1 \times 10^5$ (s ⁻¹) | $k'_2 \times 100$ (dm ³ mol ⁻¹ s ⁻¹) | Reaction Progress (%) |
|--|--|---|--------------------------|
| 2.11 | 6.19 | 57.15 | 15 |
| 3.16 | 4.50 | 43.98 | 35 |
| 4.21 | 5.13 | 36.04 | 53 |
| 5.27 | 5.32 | 30.28 | 54 |
| 6.32 | 15.83 | ... | ... |

[KMnO₄] = 4.0 × 10⁻⁴ mol dm⁻³, [Sar] = 0.05 mol dm⁻³, T = 313 K.

to 1 with respect to sarcosine for both catalytic and noncatalytic pathways [29].

Dependence of the Reaction Rate on the Sulfuric Acid Concentration

The effect of [H⁺] has been investigated by means of a series of experiments carried out at various sulfuric acid concentrations. Figure 7a is a rate–time illustration for sarcosine oxidation at various sulfuric acid concentrations. A trend of these curves indicates that as the acid concentration is raised, delay in autocatalytic behavior in the oxidation process has been increased. At high concentration of acid (about 6 mol dm⁻³), the autocatalytic effect has totally been destroyed. Such a fact can also be justified by referring to the data given in Table III. Figure 7b depicts k'_1 and k'_2 changes vs. the sulfuric acid concentration. As this figure indicates, k'_1 increases when the acid concentration is raised. The 3–3.5 mol dm⁻³ concentration region of sulfuric acid shows the least variation for k'_1 . Thus, this concentration region was determined to be the most appropriate region for the rest of our kinetic studies. In addition, it is apparent from the same figure that k'_2 decreases with the increase in the sulfuric acid concentration. Overall, it can be stated that the autocatalytic behavior of Mn²⁺ in the oxidation process also depends on the sulfuric acid concentration.

Dependence of the Reaction Rate on [MnO₄⁻]

The effect of permanganate concentration is summarized in Table IV. By paying attention to Table IV, it is obvious that k'_1 and k'_2 values are decreased with increasing initial permanganate concentration.

Table IV Rate Constants for the Catalyzed and Uncatalyzed Processes at Different Concentrations of KMnO₄

| [KMnO ₄] (mol dm ⁻³) | $k'_1 \times 10^5$ (s ⁻¹) | $k'_2 \times 100$ (dm ³ mol ⁻¹ s ⁻¹) |
|---|--|---|
| 0.0004 | 4.50 | 43.98 |
| 0.00054 | 3.68 | 38.80 |

[H₂SO₄] = 3.16 mol dm⁻³, [Sar] = 0.05 mol dm⁻³, T = 313 K.

Activation Parameters

Pseudo-order rate constants k'_1 and k'_2 at various temperatures employing Eq. (5) and at similar conditions with respect to sarcosine, sulfuric acid, and permanganate concentrations have been determined and summarized in Table I. Figures 8 and 9 demonstrate the agreement of both k'_1 and k'_2 with the Arrhenius and Eyring equations, showing linear relations with R^2 coefficients ranging from 0.991 to 0.996. Such observation is a justification of the method applied in the kinetic study of sarcosine oxidation. The activation parameters energy, enthalpy, and entropy have been obtained and are reported in Table V. Thermodynamic parameters presented in this table reveal that although the catalytic pathway requires more activation energy, the reaction rate for this pathway is more than that of the noncatalytic pathway due to large positive activation entropy. Such a fact can be further justified by calculating the activation Gibbs free energy mean values (T = 298–338 K) for catalytic and noncatalytic pathways, being equal to 79.18 and 103.38 kJ mol⁻¹, respectively.

Reaction Mechanism

In agreement with the experimental results, two separate mechanisms for the catalyzed and uncatalyzed pathways are proposed to describe the reaction pathway. Since the existence of intermediate free radicals was confirmed, their involvement in the reaction mechanism has also been considered.

Table V Activation Parameters

| Reaction Routes | E_a (kJ mol ⁻¹) | $\Delta H^\#$ (kJ mol ⁻¹) | $\Delta S^\#$ (J mol ⁻¹ K) |
|-----------------------|----------------------------------|--|--|
| Catalyzed processes | 82 (±2) ^a | 79 (±2) | -0.6(±8) |
| Uncatalyzed processes | 64 (±2) | 61 (±2) | -132(±7) |

[H₂SO₄] = 3.16 mol dm⁻³, [KMnO₄] = 4.0 × 10⁻⁴ mol dm⁻³, [Sar] = 0.05 mol dm⁻³, T = 298–318 K.

^a Values in parenthesis are estimated errors on each parameter.

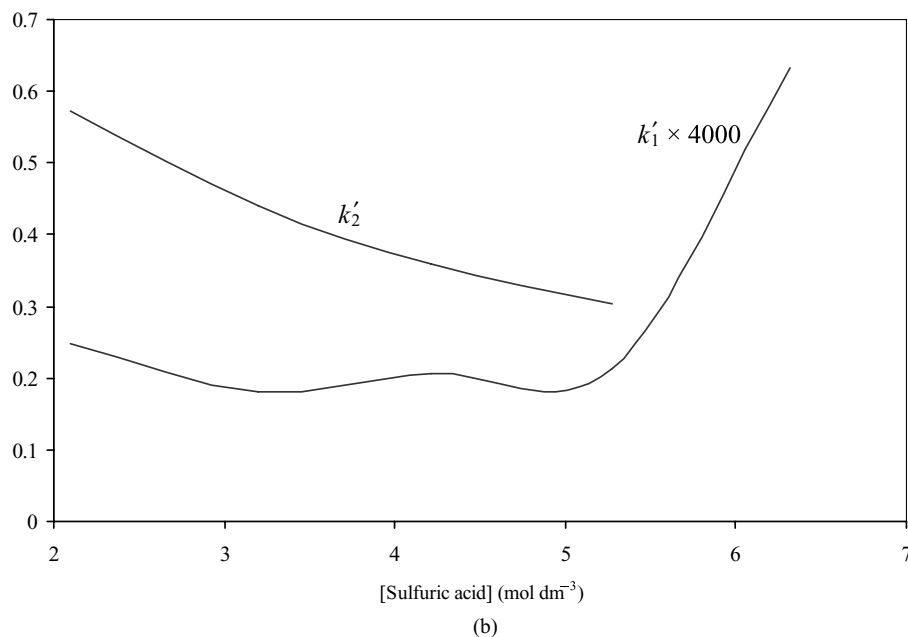
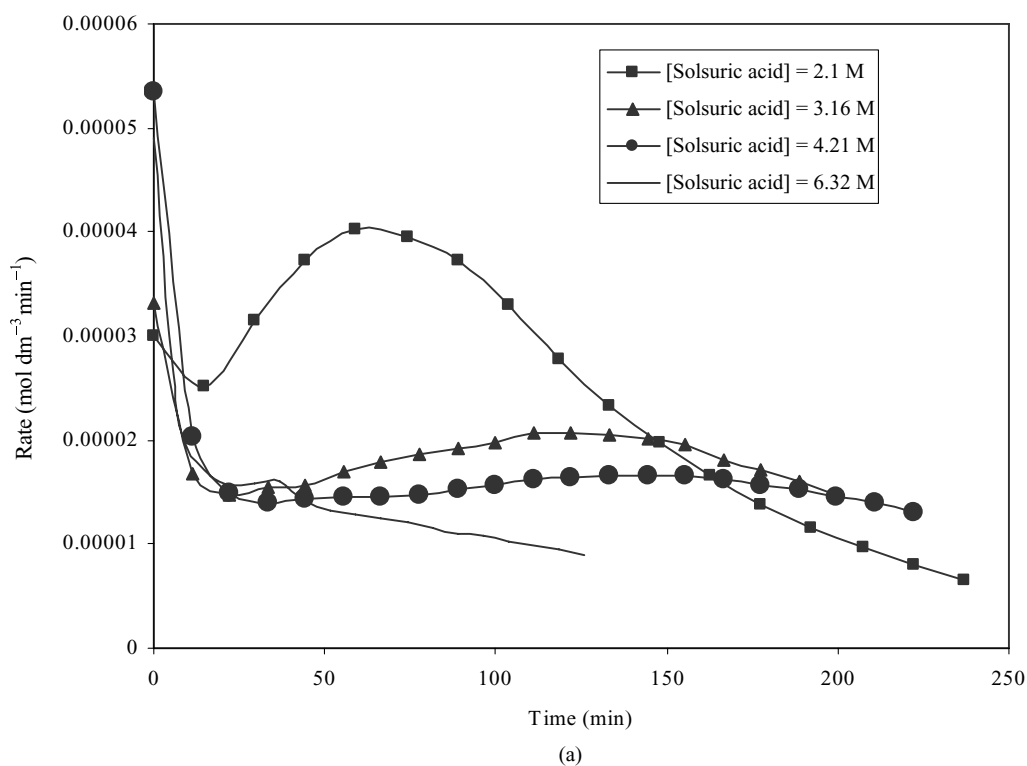


Figure 7 Effect of the sulfuric acid concentration on (a) the reaction rate–time plots and (b) the catalyzed and uncatalyzed pseudo-order rate constants. $[\text{KMnO}_4] = 4.0 \times 10^{-4} \text{ mol dm}^{-3}$, $[\text{Sar}] = 0.05 \text{ mol dm}^{-3}$, $T = 313 \text{ K}$; $k'_1 \text{ (s}^{-1}\text{)}$, $k'_2 \text{ (dm}^3 \text{ mol}^{-1} \text{ s}^{-1}\text{)}$.

Reaction Mechanism for the Uncatalyzed Process.

All the experiments were performed in moderately concentrated sulfuric acid media and are considered as acid-catalyzed reactions. Therefore, it is expected

that H^+ may be consumed and later generated in various steps. With the evidence presented pointing to no involvement of other manganese ions except Mn(VII) in the sarcosine oxidation process, the latter

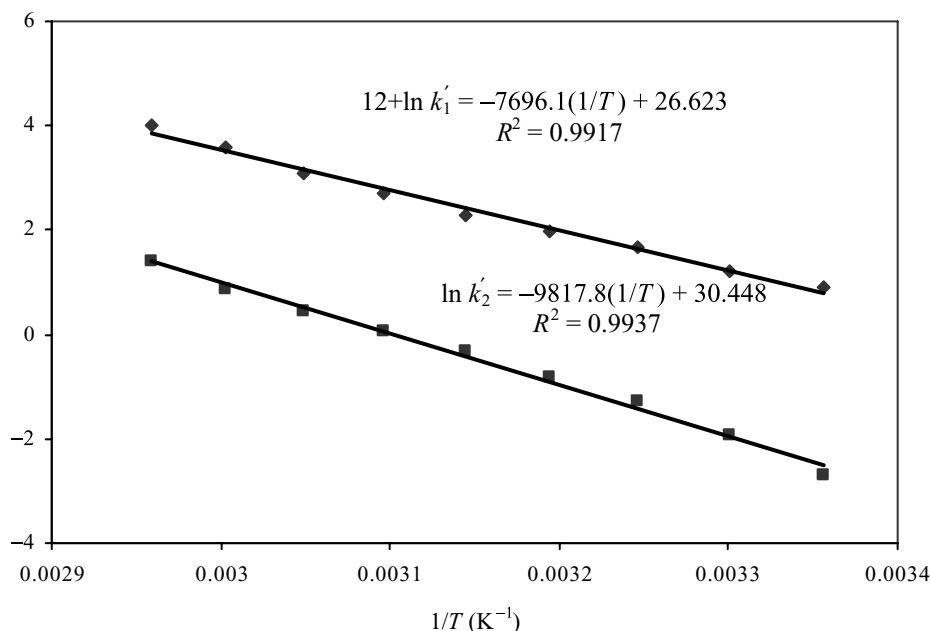
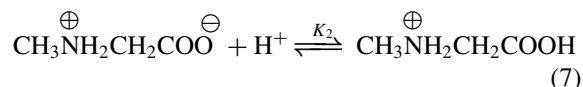


Figure 8 Arrhenius plots for the catalyzed and uncatalyzed processes. $[\text{KMnO}_4] = 4.0 \times 10^{-4} \text{ mol dm}^{-3}$, $[\text{H}_2\text{SO}_4] = 3.16 \text{ mol dm}^{-3}$, $[\text{Sar}] = 0.05 \text{ mol dm}^{-3}$.

ion is the most probable reactive species. The reaction rate enhancement observed by increasing acid concentration suggests the formation of a more powerful oxidant, namely permanganic acid, by the following equilibrium:



At the high acid concentration used, protonation of the zwitterionic form of sarcosine gives



A mechanism consistent with the observed kinetic data includes the following steps: In agreement with the

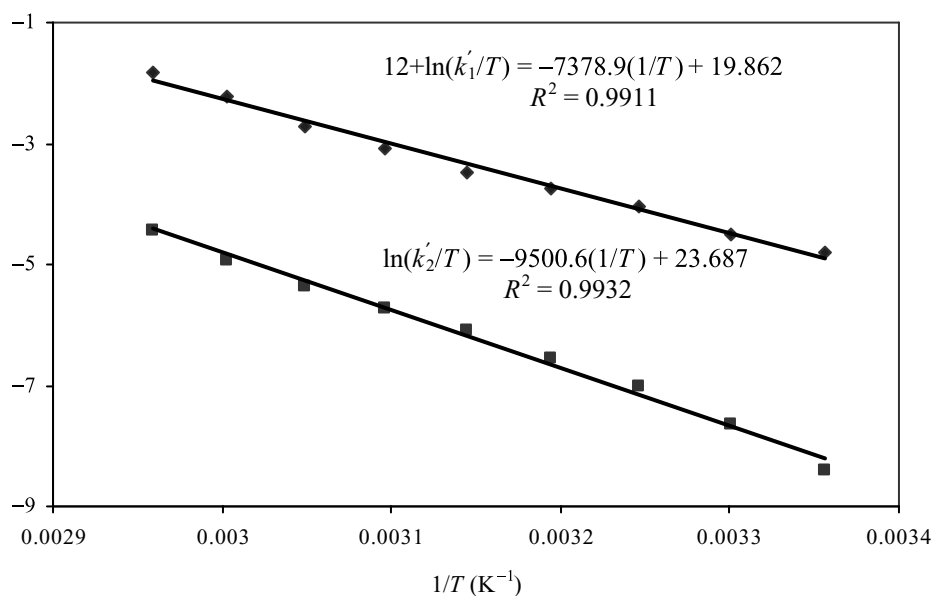


Figure 9 Eyring plots for the catalyzed and uncatalyzed processes. $[\text{KMnO}_4] = 4.0 \times 10^{-4} \text{ mol dm}^{-3}$, $[\text{H}_2\text{SO}_4] = 3.16 \text{ mol dm}^{-3}$, $[\text{Sar}] = 0.05 \text{ mol dm}^{-3}$.

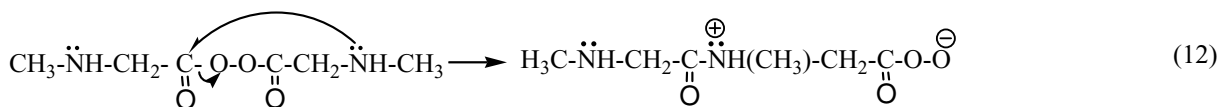
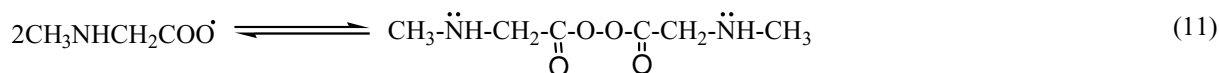
experimental results, the formation of an addition complex between the permanganic acid and the cationic form of the sarcosine is proposed [28,29,53].



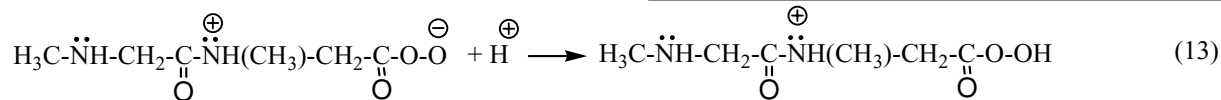
This complex may rupture according to the following equation:



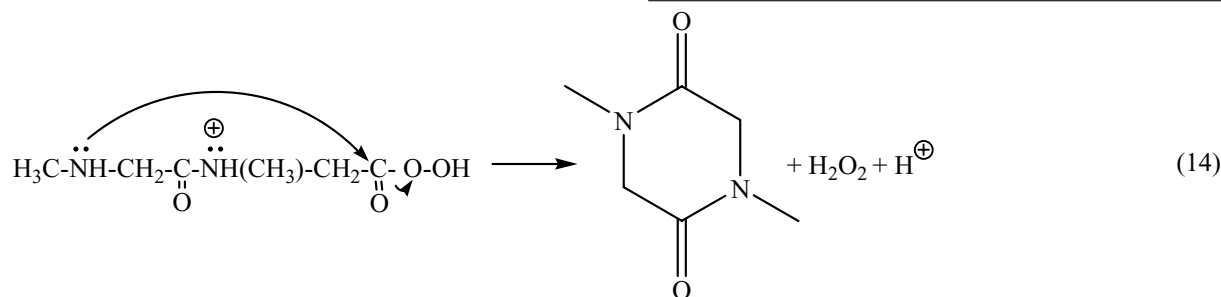
Based on the radical involvement in the reaction mechanism, a dimer species is formed by the following steps:



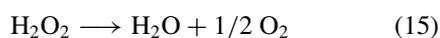
To have an appropriate leaving group, the following step may be considered:



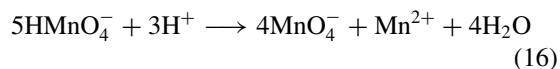
Owing to an internal rearrangement of the aforementioned dimer, a product involving the diketopiperazine skeleton is finally produced.



Hydrogen peroxide decomposition can be considered as follows:



Knowing the fact that the species Mn(VI) is very unstable in strong acidic media, it will be converted into Mn(II) and Mn(VII) by means of a rapid disproportionation.



Multiplying Eqs. (6)–(10) by a factor of 10, Eqs. (11)–(15) by a factor of 5, Eq. (16) by a factor of 2, and then summing them with each other results in the satisfaction of the overall reaction with the stoichiometry. In agreement with the above scheme, assuming a steady-state approximation for X_1^+ , the rate equation obtained for the uncatalyzed process is

$$-\frac{d[\text{Mn(VII)}]}{dt} = k'_1[\text{MnO}_4^-] \quad (17)$$

$$k'_1 = \frac{\alpha_0[\text{Sar}]_t[\text{H}^+]^2}{\beta_0(1 + \beta_1[\text{H}^+] + \beta_2[\text{H}^+]^2) + \alpha_1[\text{H}^+]^2[\text{Mn(VII)}]} \quad (18)$$

$$\begin{aligned} \alpha_0 &= K_1 K_2 k_3 k_4 \\ \alpha_1 &= K_1 K_2 k_3 \\ \beta_0 &= k_{-3} + k_4 \end{aligned}$$

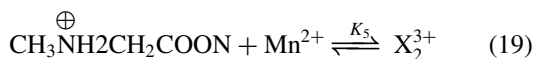
$$\beta_1 = K_1 + K_2$$

$$\beta_2 = K_1 K_2$$

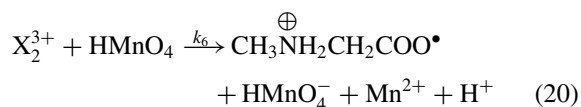
where $[\text{Sar}]_t$ represents the total concentration of sarcosine and $[\text{Mn(VII)}]$ represents the total concentration of permanganate.

The rate law obtained above corresponds to that mechanism explaining the observed experimental behavior: the first-order reaction with respect to permanganate and sarcosine concentrations, and change in k'_1 , the uncatalyzed pseudo-order rate constant when the initial permanganate concentration varies.

Reaction Mechanism for the Catalyzed Process. Addition of Mn^{2+} ions led to an increase in the reaction rate, while the evidence presented also suggests that an adduct might be formed between Mn^{2+} and the protonated sarcosine.



As the rate-determining step, a slow attack of permanganic acid to the above-mentioned complex has been proposed [48,53].



The remaining steps, leading to the final products, resemble those presented for the uncatalyzed pathway. Again, multiplying Eqs. (6), (7), (19), (20), (10), by a factor of 10, Eqs. (11)–(15) by a factor of 5, Eq. (16) by a factor of 2, and then summing them with each other results in the overall reaction's equation with the correct stoichiometry. Assuming a steady-state approximation for the X_2^{3+} complex in the above mechanism, the following rate equation [53] is derived:

$$-\frac{d[\text{Mn(VII)}]}{dt} = k'_1[\text{MnO}_4^-] + k'_2[\text{MnO}_4^-][\text{Mn}^{2+}] \quad (21)$$

$$k'_2 = \frac{\beta_0 \delta_0 [\text{Sar}]_t [\text{H}^+]^2}{\beta_0 (1 + \beta_1 [\text{H}^+] + [\text{H}^+]^2) + \alpha_1 [\text{H}^+]^2 [\text{Mn(VII)}] + \beta_0 \delta_1 [\text{H}^+] [\text{Mn}^{2+}] + \beta_0 \delta_2 [\text{H}^+]^2 [\text{Mn}^{2+}]} \quad (22)$$

$$\delta_0 = K_1 K_2 K_5 k_6$$

$$\delta_1 = K_2 K_5$$

$$\delta_2 = K_1 K_2 K_5$$

where the notation employed in Eq. (17) is conserved.

This rate law is in accord with all experimental results presented in this article, namely the first-order dependence on Mn^{2+} ions, permanganate ions, and sarcosine concentrations and the change in k'_2 values with respect to the initial permanganate concentration.

Owing to the complexity of the proposed mechanism, evaluation of the rate constant values corresponding to the reaction rate-determining steps for both processes has not been possible. Thus, the activation parameters reported are associated with reaction pseudo-rate constants k'_1 and k'_2 , and these values cannot be attributed to any particular reaction step.

CONCLUSIONS

To study the influence of substitution on the amine functional group of glycine in oxidation of such α -amino acids, the kinetics of permanganate oxidation reaction with sarcosine in a moderately concentrated sulfuric acid medium was investigated using a spectrophotometric technique. The present work is concerned with the crucial evidence for the cyclization of two sarcosine molecules, which is being reported for the first time. To the best of our knowledge, there is no report in the literature for the oxidation of this amino acid and preparation of DKPs via oxidation of a secondary α -amino acid with KMnO_4 in water media. It is well known that oxidation of primary α -amino acids with KMnO_4 in water produces simple aldehydes. Here, by using a secondary α -amino acid instead and having the same conditions, an interesting product was encountered, namely 1,4-dimethylpiperazine-2,5-dione. The well-known and important DKP obtained in a single step preparation was completely characterized by IR, mass, ^1H NMR, and ^{13}C NMR spectral analyses, as well as its melting point.

Other major goals of this paper are to replace environmentally unfriendly organic solvents with environmentally friendly H_2O , to omit organic solvents, and

to increase reaction rates and product yields. By investigating rate–time curves, it is concluded that when a

determined portion of the reaction time for sarcosine has passed, a parallel reaction is encountered similar to that of primary α -amino acids studied in our previous works. Results show that this process can be considered as a delayed autocatalytic reaction. By increasing the concentration of Mn(II), speeding the reaction, and also fitting the kinetics data into appropriate kinetics equations, it is determined that this species is the autocatalytic agent. It has been determined that the initiation of autocatalytic activity depends not only on the Mn²⁺ concentration but also on that of sarcosine. Thus, the delayed autocatalytic effect can occur only at a certain concentration of Mn²⁺ to sarcosine, namely the "critical ratio." Moreover, the delayed autocatalytic phenomenon in such reactions vanishes in concentrations of sulfuric acid that are greater than 6 M. Therefore, it is appropriate to conclude that the mentioned phenomenon depends on the amount of sulfuric acid in the medium.

The pseudo-order rate constants obtained for both the catalytic and noncatalytic pathways when sarcosine was in excess obeyed the Arrhenius and Eyring relations. The activation parameters associated with reaction pseudo-rate constants k'_1 and k'_2 were computed and discussed. It is clear that results obtained in the present work satisfy the presence of radical intermediates as well as the formation and decomposition of permanganate–sarcosine and Mn²⁺–sarcosine complexes in these reactions.

Based on above facts, plausible mechanisms for catalytic and noncatalytic pathways involving the formation of a dipeptide between two sarcosine molecules have been proposed and discussed. The rate laws derived are in excellent agreement with the experimental results.

Our special thanks to Dr. Khosrow Jadidi and Mr. Abbas Rahmati for their valuable insights.

BIBLIOGRAPHY

- Willie, A.; Edmondson, D. E.; Jorns, M. S. *Biochemistry* 1996, 35, 5292.
- Wagner, M. A.; Jorns, M. S. *Biochemistry* 2000, 39, 8825.
- Chen, Z.; Zhao, G.; Martinovic, S.; Jorns, M. S.; Mathews, F. S. *Biochemistry* 2005, 44, 15444.
- Wagner, M. A.; Khanna, P.; Jorns, M. S. *Biochemistry* 1999, 38, 5588.
- Siwicka, K. W.; Rosiek, B.; Leniewski, A.; Maurin, J. K.; Czarnocki, Z. *Tetrahedron: Asymmetry* 2005, 16, 975.
- Parrish, D. A.; Mathias, L. J. *J Org Chem* 2002, 67, 1820.
- Khimiuk, A. Y.; Korennykh, A. V.; van Langen, L. M.; van Rantwijk, F. *Tetrahedron: Asymmetry* 2005, 16, 975.
- Poullennec, G.; Romo, D. *J Am Chem Soc* 2003, 125, 6344.
- Nakamura, D.; Kakiuchi, K.; Koga, K.; Shirai, R. *Org Lett* 2006, 8, 6139.
- Poullennec, K. G.; Kelly, A. T.; Romo, D. *Org Lett* 2002, 4, 2645.
- Ishihara, K.; Ohara, S.; Yamamoto, H. *J Org Chem* 1996, 61, 4196.
- Porzi, G.; Sandri, S. *Tetrahedron: Asymmetry* 1994, 5, 453.
- Sanner, M. A.; Weigelt, C.; Stansberry, M.; Killen, K.; Michne, W. F.; Kessler, D. W.; Kulling, R. K. *J Org Chem* 1992, 57, 5264.
- Ma, X.; Zhao, Y. *J Org Chem* 1989, 54, 4005.
- Zahedi, M.; Bahrami, H. *Kinet Catal* 2004, 45, 351.
- Bahrami, H.; Zahedi, M. *Can J Chem* 2004, 82, 1.
- Bahrami, H.; Zahedi, M. *Int J Chem Kinet* 2006, 38, 1.
- Verma, R. S.; Reddy, M. J.; Shastry, R. *J Chem Soc, Perkin Trans* 1976, 2, 469.
- Frost, A. A.; Pearson, R. G. *Kinetic and Mechanisms*; Wiley: New York, 1972; p 152.
- Ameta, C. S.; Pande, P. N.; Gupta, H. L.; Chowhhry, H. C. *Acta Phys Chem* 1980, 26, 89.
- Ameta, C. S.; Pande, P. N.; Gupta, H. L.; Chowhhry, H. C. *Z Phys Chem (Leipzig)* 1980, 261, 1222.
- Ameta, C. S.; Pande, P. N.; Gupta, H. L.; Chowhhry, H. C. *Z Phys Chem (Leipzig)* 1980, 261, 802.
- Ameta, C. S.; Pande, P. N.; Gupta, H. L.; Chowhhry, H. C. *Acta Chim Acad Sci Hung* 1982, 110, 7.
- Bharadwaj, L. M.; Nigam, P. C. *Ind J Chem Ser A* 1981, 8, 793.
- Rao, V. S.; Sethuram, B.; Rao, T. N. *Int J Chem Kinet* 1979, 11, 165.
- Rao, V. S.; Sethuram, B.; Rao, T. N. *Oxid Commun* 1986, 9, 11.
- Mudaliar, U. D.; Chourey, V. R.; Verma, R. S.; Shastry, V. R. *Ind J Chem Soc* 1983, 60, 561.
- Girgis, H. M.; Hassan, R. M.; El-Shahawy, A. S. *Bull Fac Sci Univ* 1987, 16(1), 41.
- Hassan, R. M.; Mousa, M. A.; Wahdan, M. H. *J Chem Soc, Dalton Trans* 1988, 3, 605.
- Iloukani, H.; Bahrami, H. *Int J Chem Kinet* 1999, 31, 95.
- Sahu, B. R.; Chourey, V. R.; Pandey, S.; Shastry, L. V.; Shastry, V. R. *Ind J Chem Soc* 2000, 76, 131.
- Vogel, A. I. *Quimica Analitica Cuantitativa*; Kapelus: Buenos Aires, Argentina, 1960; Vol I, p 382.
- Banerji, K. K.; Nath, P. *Bull Chem Soc Japan* 1969, 42, 2038.
- Stewart, R.; Gardner, K. A.; Kuehnert, L. L.; Mayer, J. M. *Inorg Chem* 1997, 107, 4220.
- Andrés Ordax, F. J.; Arrizabalaga, A.; Martínez de Ilarduya, J. I. *An Quim* 1984, 80, 531.

36. Andrés Ordax, F. J.; Arrizabalaga, A.; Martínez Pérez de mendiola, R. *Studia Chem* 1986, 11, 303.
37. Andrés Ordax, F. J.; Arrizabalaga, A.; Ortega, K. *An Quim* 1989, 85, 218.
38. Pérez Benito, J. F.; Mata Pérez, F.; Brillas, E. *Can J Chem* 1987, 65(10), 2329.
39. Brillas, E.; Garrido, J. A.; Pérez Benito, J. F. *Collect Czech Chem Comun* 1988, 53, 479.
40. Garrido, J. A.; Pérez Benito, J. F.; Rodrigouez, R. M.; De Andrés, J.; Brillas, E. *J Chem Res* 1987, 11, 380.
41. De Andrés, J.; Brillas, E.; Garrido, J. A.; Pérez Benito, J. F. *J Chem Soc, Perkin Trans* 1988, 2, 107.
42. Rodríguez, R. M.; De Andrés, J.; Brillas, E.; Garrido, J. A.; Pérez Benito, J. F. *New J Chim* 1988, 2(2), 143.
43. De Andrés, J.; Brillas, E.; Garrido, J. A.; Pérez Benito, J. F. *Gazz Ital* 1988, 118, 203.
44. Kovacs, K. A.; Grof, P.; Burai, L.; Riedel, M. *J Phys Chem A* 2004, 108, 11026.
45. Waters, W. A. *Q Rev Chem Soc* 1958, 12, 277.
46. Ganapathisubramanian, N. *J Phys Chem* 1988, 92, 414.
47. Powell, R. T.; Oskin, T.; Ganapathisubramanian, N. *J Phys Chem* 1989, 93, 2718.
48. Arrizabalaga, F. J.; Andrés Ordax, M. Y.; Fernández Aránguiz, R. *Peche Int J Chem Kinet* 1997, 29, 181.
49. Andrés Ordax, F. J.; Arrizabalaga, A.; Casado, J.; Peche, R. *React Kinet Catal Lett* 1991, 44, 293.
50. Andrés Ordax, F. J.; Arrizabalaga, A.; Peche, R.; Quintana, M. A. *An Quim* 1992, 87, 828.
51. Andrés Ordax, F. J.; Arrizabalaga, A.; Peche, R.; Quintana, M. A. *An Quim* 1992, 88, 440.
52. Insausti, M. J.; Mata-Pérez, F.; Alvarez-Macho, M. P. *Int J Chem Kinet* 1995, 27, 507.
53. Arrizabalaga, F. J.; Andrés Ordax, M. Y.; Fernández Aránguiz, R. P. *Int J Chem Kinet* 1996, 28, 799.